Hindawi Publishing Corporation
Bioinorganic Chemistry and Applications
Volume 2015, Article ID 717089, 14 pages
http://dx.doi.org/10.1155/2015/717089

Research Article

Synthesis and Characterization of Bioactive Acylpyrazolone Sulfanilamides and Their Transition Metal Complexes: Single Crystal Structure of 4-Benzoyl-3-methyl-1-phenyl-2-pyrazolin-5-one Sulfanilamide

Omoruyi G. Idemudia,[1] Alexander P. Sadimenko,[1] Anthony J. Afolayan,[2] and Eric C. Hosten[3]

[1]*Chemistry Department, University of Fort Hare, Private Bag X1314, Alice 5700, South Africa*
[2]*Botany Department, University of Fort Hare, Private Bag X1314, Alice 5700, South Africa*
[3]*Chemistry Department, Nelson Mandela Metropolitan University, P.O. Box 77000, Port Elizabeth 6031, South Africa*

Correspondence should be addressed to Omoruyi G. Idemudia; oidemudia@ufh.ac.za

Received 11 April 2015; Accepted 25 April 2015

Academic Editor: Claudio Pettinari

Copyright © 2015 Omoruyi G. Idemudia et al. This is an open access article distributed under the Creative Commons Attribution License, which permits unrestricted use, distribution, and reproduction in any medium, provided the original work is properly cited.

Two Schiff base ligands Ampp-Sn **1** and Bmpp-Sn **2**, afforded by a condensation reaction between sulfanilamide and the respective acylpyrazolone carbonyl precursors, their Mn(II), Co(II), Ni(II), and Cu(II) complexes prepared by the reaction of ligands and corresponding metal salts in aqueous solutions, were synthesized and then characterized by both analytical and spectroscopic methods, in a view to developing new improved bioactive materials with novel properties. On the basis of elemental analysis, spectroscopic and TGA results, transition metal complexes, with octahedral geometry having two molecules of the bidentate keto-imine ligand each, have been proposed. The single crystal structure of Bmpp-Sn according to X-ray crystallography showed a keto-imine tautomer type of Schiff base, having three intramolecular bonds, one short N2⋯H2⋯O3 hydrogen bond of 1.90 Å and two long C13⋯H13⋯O2 and C32⋯H32⋯O3 hydrogen bonds of 2.48 Å. A moderate to low biological activities have been exhibited by synthesized compounds when compared with standard antimicrobial agents on screening the synthesized compounds against *Staphylococcus aureus*, *Bacillus pumilus*, *Proteus vulgaris*, and *Aeromonas hydrophila* for antibacterial activity and against free radical 1, 1-diphenyl-2-picryl-hydrazyl (DPPH) for antioxidant activity.

1. Introduction

The electrophilic carbonyl carbon in aldehydes and ketones is a target site for nucleophilic primary amines to form an interesting group of ligands known as Schiff bases *via* a condensation reaction. Schiff bases possess remarkable reactivity and properties which have been observed to be more efficient when in coordination with transition metals, hence their diverse applications [1–8]. Acylpyrazolones are a series of heterocyclic diketones that have attracted a lot of research attention because of their chemistry and strong chelating properties especially towards transition metal ions [9] and numerous uses [10]. Knorr first synthesized pyrazolone derivatives by reacting phenyl hydrazine with ethylacetoacetate to form a novel 1-phenyl-3-methyl-5-pyrazolone in 1883 and studies on this group of compounds have been on since then [11]. They have the ability to exist either in an enol or keto tautomer forms, which gives them the potential to form different types of interesting coordination compounds [12, 13]. Sulfanilamides are the simplest of the family of sulfa drugs. They act as metabolites capable of obstructing folic acid synthesis in bacteria, thereby causing cell death, the reason for their strong antibacterial activity [14]. There has been hypothesis that some metal complexes of sulphur containing ligands have shown more potency in their anticancer properties [15, 16]. Coombs and coworkers synthesized Schiff bases of

sulfanilamide with salicylaldehyde and their palladium complexes [14]. The single crystal structure of another salicylaldehyde Schiff base, N, N′-(*p*-phenyl sulfanilamide)-5,6-dimethoxypyrimidine-(2-hydroxyl benzene) methylidene, with excellent fluorescent properties has also been resolved [17]. We have reported the X-ray crystal and molecular structures of 4-benzoyl derivatives Schiff bases, 4-benzoyl-3-methyl-1-phenyl-2-pyrazolin-5-one phenylhydrazone [18] and 4-benzoyl-3-methyl-1-phenyl-2-pyrazolin-5-one-2,4-dinitrophenylhydrazone [19]. In continuation of our probe on new Schiff bases and taking the advantage of possible synergistic properties from the combination of acylpyrazolone and sulfanilamide, presented herein are the synthesis, characterization, antibacterial and antioxidant studies of 4-acylpyrazone with 4-aminobenzenesulfonamide Schiff bases and their Mn(II), Co(II), Ni(II), and Cu(II) complexes.

2. Experimental

2.1. Materials and Methods. Melting point was determined using the GallenKamp melting point apparatus. CHN elemental analyses were carried out on a LECO.TRUSpec Micro CHNS analyzer. FTIR spectra were measured as KBr Pellets (4000–370 cm^{-1}) on a Perkin-Elmer Model System 2000 FTIR spectrophotometer. Electronic spectra of metal complexes were recorded on a Perkin-Elmer Lambda 25 spectrophotometer and a Sherwood Scientific magnetic susceptibility balance was used for magnetic moments with powder samples of complexes at room temperature. Diamagnetism corrections were estimated from Pascal's constants. ^{1}H and ^{13}C NMR spectra in deuterated DMSO were recorded on a Bruker 600 MHz Avance II NMR spectrophotometer using trimethylsilane TMS, as internal standard. Chemical shifts are given in ppm (δ scale). Thermal analyses were done on a NETZSCH STA 449 C instrument at a temperature range of 20–900°C with a heating rate of 20°C min^{-1} in nitrogen gas. Mass spectra of ligands were determined by the Bruker micrOTOF-Q II 10390 mass spectrometer. They were analyzed with ACPI using a direct insertion probe (DIP). An external calibration with sodium formate was performed to attain the correct accurate mass. Single crystal X-ray diffraction studies were performed at 200 K using a Bruker Kappa Apex II diffractometer with graphite monochromated Mo Kα radiation (λ = 0.71073 Å). All reagents, Manganese(II) chloride tetrahydrate $MnCl_2{\cdot}4H_2O$, Cobalt(II) chloride hexahydrate $CoCl_2{\cdot}6H_2O$, Nickel(II) chloride hexahydrate $NiCl_2{\cdot}6H_2O$, Copper(II) acetate monohydrate $(CH_3COO)_2Cu{\cdot}H_2O$, sulfanilamide, and 3-methyl-1-phenyl-2-pyrazolin-5-one, and solvents were of analytical grade as supplied by Aldrich. Schiff base precursors 4-acyl-3-methyl-1-phenyl-2-pyrazolin-5-one derivatives were synthesized and purified as reported earlier [20].

2.2. General Procedure for the Synthesis of Acylpyrazolone Schiff Bases. To a solution of 4-benzoyl-3-methyl-1-phenyl-2-pyrazolin-5-one (2.0 mmol, 0.56 g) and 4-acetyl-3-methyl-1-phenyl-2-pyrazolin-5-one (2.0 mmol, 0.43 g) in methanol (40 mL) each in a separate round bottom flask sulfanilamide was added in drops (2.0 mmol, 0.34 g) in hot methanol while stirring; Bmpp-Sn and Ampp-Sn were precipitated, respectively, after 4 h of reflux. The resulting yellow (Bmpp-Sn) and pale-yellow (Ampp-Sn) solids were filtered, washed with methanol, and dried at room temperature. They were recrystallized from methanol and stored over fused $CaCl_2$. Suitable thread-like yellow single crystals of Bmpp-Sn for X-ray diffraction were grown at room temperature from slow evaporation of methanol solution after seven days.

*2.2.1. 4-Acetyl-3-methyl-1-phenyl-2-pyrazolin-5-one Sulfanilamide: Ampp-Sn (**1**).* Pale yellow solid, yield 74%, mp 232–234°C; IR KBr (ν_{max}, cm^{-1}): 3496 (N–H), 2954 (C–H), 1633 (C=N), 1503 (C=O). ^{1}H NMR (600 MHz, DMSO): δ (ppm) 13.1 (s, 1H, –NH), 8.0 (s, 1H, C=N–H), 7.9–7.2 (m, 9H, aromatic–H), 2.4 (s, 3H, CH_3). ^{13}C NMR (600 MHz, DMSO): δ (ppm) 165.4 (s, C=O), 164.5 (s, C=N), 148.2 (s, C–S) 142.8–116.6 (s, aromatic carbons), 17.6 (s, pyrazolone CH_3), 17.5 (s, acetyl CH_3); APCI-MS: *m*/*z* 371.11 ($[M + H]^+$, 100%). Anal. Calcd. $C_{18}H_{18}N_4O_3S$ (370.11): C, 58.36; H, 4.90; N, 15.13%. Found: C, 58.42; H, 4.88; N, 15.18%.

*2.2.2. 4-Benzoyl-3-methyl-1-phenyl-2-pyrazolin-5-one Sulfanilamide: Bmpp-Sn (**2**).* Yellow solid, yield 69%, mp 102–104°C; IR KBr (ν_{max}, cm^{-1}): 3497 (N–H), 2927 (C–H), 1639 (C=N), 1504 (C=O). ^{1}H NMR (600 MHz, DMSO): δ (ppm) 12.8 (br, 1H, –NH), 8.0 (s, 1H, C=N–H), 7.8–7.1 (m, 14H, aromatic–H), 2.2 (s, 3H, CH_3). ^{13}C NMR (600 MHz, DMSO): δ (ppm) 190.5 (s, C=O), 139.3 (s, C=N), 148.2 (s, C–S) 132.2–110.7 (s, aromatic carbons), 16.5 (s, pyrazolone CH_3); APCI-MS: *m*/*z* 433.13 ($[M + H]^+$, 100%). Anal. Calcd. $C_{23}H_{20}N_4O_3S$ (432.13): C, 63.87; H, 4.66; N, 12.96%. Found: C, 63.84; H, 4.67; N, 12.79%.

2.3. General Procedure for the Synthesis of Acylpyrazolone Schiff Bases Metal Complexes. To a solution of Bmpp-Sn (2 mmol, 0.87 g) and Ampp-Sn (2 mmol, 0.74 g) in hot ethanol (40 mL) each in a separate round bottom flask aqueous solution of 2 mmol of corresponding metal salts was added in drops while stirring under reflux and followed by the addition of NaOH (2 mmol, 0.08 g) to precipitate the metal complex. After 4 h of reflux, the precipitates in different colours were filtered, washed with ethanol/water (1 : 1), dried at room temperature, and stored over fused $CaCl_2$.

*2.3.1. Bis(4-acetyl-3-methyl-1-phenyl-2-pyrazolin-5-one sulfanilamide)diaquamanganese(II) Monohydrate Mn(Ampp-Sn)$_2$(H_2O)$_2$·H_2O (**1a**).* Yellow solid; yield 81%; mp 210–212°C; Molar cond. (10^{-3} M in DMF): 14.40 ohm^{-1} cm^2 mol^{-1}; μ_{eff} (B.M.): 5.61; UV-Vis (DMF) λ_{max} nm: 259 ($\pi \rightarrow \pi^*$), 377 ($n \rightarrow \pi^*$), 431 ($d \rightarrow d$); IR KBr (ν_{max}, cm^{-1}): 3484 (N–H), 3392 (O–H), 2920 (C–H), 1624 (C=N), 824 (H_2O), 634 (M–N), 488 (M–O); Anal. Calcd. $C_{36}H_{40}N_8O_9S_2Mn$ (847.17): C 50.99, H 4.76, N 13.22%, Found: C 51.01, H 4.58, N 13.21%.

*2.3.2. Bis(4-acetyl-3-methyl-1-phenyl-2-pyrazolin-5-one sulfanilamide)diaquacobalt(II) Co(Ampp-Sn)$_2$(H_2O)$_2$ (**1b**).* Yellow

solid; yield 82%; mp 150–151°C; Molar cond. (10^{-3} M in DMF): 11.22 ohm^{-1} cm^2 mol^{-1}; μ_{eff} (B.M.): 4.43; UV-Vis (DMF) λ_{max} nm: 274 ($\pi \rightarrow \pi^*$), 377 (n $\rightarrow \pi^*$), 408, 632, 699 (d $\rightarrow$ d); IR KBr (ν_{max}, cm^{-1}): 3491 (N–H), 3391 (O–H), 2923 (C–H), 1619 (C=N), 831 (H_2O), 631 (M–N), 486 (M–O); Anal. Calcd. $C_{36}H_{38}N_8O_8S_2Co$ (833.16): C 51.85, H 4.60, N 13.45%, Found: C 51.61, H 4.51, N 13.11%.

*2.3.3. Bis(4-acetyl-3-methyl-1-phenyl-2-pyrazolin-5-one sulfanilamide)diaquanickel(II) Monohydrate Ni(Ampp-Sn)$_2$(H_2O)$_2$·H_2O (**1c**).* Yellow solid; yield 79%; mp 157–158°C; Molar cond. (10^{-3} M in DMF): 16.02 ohm^{-1} cm^2 mol^{-1}; μ_{eff} (B.M.): 2.93; UV-Vis (DMF) λ_{max} nm: 257 ($\pi \rightarrow \pi^*$), 324 (n $\rightarrow \pi^*$), 596, 674 (d $\rightarrow$ d); IR KBr (ν_{max}, cm^{-1}): 3488 (N–H), 3398 (O–H), 2934 (C–H), 1620 (C=N), 823 (H_2O), 622 (M–N), 488 (M–O); Anal. Calcd. $C_{36}H_{40}N_8O_9S_2Ni$ (850.93): C 50.77, H 4.74, N 13.16%, Found: C 50.65, H 4.71, N 13.30%.

*2.3.4. Bis(4-acetyl-3-methyl-1-phenyl-2-pyrazolin-5-one sulfanilamide)diaquacopper(II) Monohydrate Cu(Ampp-Sn)$_2$(H_2O)$_2$·H_2O (**1d**).* Yellow solid; yield 83%; mp 298–299°C; Molar cond. (10^{-3} M in DMF): 7.04 ohm^{-1} cm^2 mol^{-1}; μ_{eff} (B.M.): 1.90; UV-Vis (DMF) λ_{max} nm: 261 ($\pi \rightarrow \pi^*$), 365 (n $\rightarrow \pi^*$), 618, (d $\rightarrow$ d); IR KBr (ν_{max}, cm^{-1}): 3482 (N–H), 3392 (O–H), 2922 (C–H), 1617 (C=N), 850 (H_2O), 628 (M–N), 498 (M–O); Anal. Calcd. $C_{36}H_{40}N_8O_9S_2Cu$ (855.78): C 50.48, H 4.71, N 13.09%, Found: C 50.44, H 4.59, N 13.21%.

*2.3.5. Bis(4-benzoyl-3-methyl-1-phenyl-2-pyrazolin-5-one sulfanilamide)diaquamanganese(II) Mn(Bmpp-Sn)$_2$(H_2O)$_2$ (**2a**).* Pale yellow solid; yield 82%; mp 180–182°C; Molar cond. (10^{-3} M in DMF): 8.19 ohm^{-1} cm^2 mol^{-1}; μ_{eff} (B.M.): 5.82; UV-Vis (DMF) λ_{max} nm: 277 ($\pi \rightarrow \pi^*$), 378 (n $\rightarrow \pi^*$), 424, 589 (d $\rightarrow$ d); IR KBr (ν_{max}, cm^{-1}): 3483 (N–H), 3398 (O–H), 2938 (C–H), 1623 (C=N), 844 (H_2O), 619 (M–N), 470 (M–O); Anal. Calcd. $C_{46}H_{42}N_8O_8S_2Mn$ (953.19): C 57.91, H 4.44, N 11.75%, Found: C 57.72, H 4.14, N 11.22%.

*2.3.6. Bis(4-benzoyl-3-methyl-1-phenyl-2-pyrazolin-5-one sulfanilamide)diaquacobalt(II) Monohydrate Co(Bmpp-Sn)$_2$(H_2O)$_2$·H_2O (**2b**).* Pink solid; yield 89%; mp 144–146°C; Molar cond. (10^{-3} M in DMF): 10.30 ohm^{-1} cm^2 mol^{-1}; μ_{eff} (B.M.): 4.46; UV-Vis (DMF) λ_{max} nm: 262 ($\pi \rightarrow \pi^*$), 376 (n $\rightarrow \pi^*$), 408, 540 (d $\rightarrow$ d); IR KBr (ν_{max}, cm^{-1}): 3492 (N–H), 3398 (O–H), 2925 (C–H), 1618 (C=N), 849 (H_2O), 624 (M–N), 489 (M–O); Anal. Calcd. $C_{46}H_{44}N_8O_9S_2Co$ (975.20): C 56.60, H 4.55, N 11.49%, Found: C 56.33, H 4.92, N 11.16%.

*2.3.7. Bis(4-benzoyl-3-methyl-1-phenyl-2-pyrazolin-5-one sulfanilamide)diaquanickel(II) Monohydrate Ni(Bmpp-Sn)$_2$(H_2O)$_2$·H_2O (**2c**).* Light green solid; yield 85%; mp 190–192°C; Molar cond. (10^{-3} M in DMF): 11.62 ohm^{-1} cm^2 mol^{-1}; μ_{eff} (B.M.): 2.89; UV-Vis (DMF) λ_{max} nm: 278 ($\pi \rightarrow \pi^*$), 377 (n $\rightarrow \pi^*$), 410, 683 (d $\rightarrow$ d); IR KBr (ν_{max}, cm^{-1}): 3489 (N–H), 3390 (O–H), 2935 (C–H), 1619 (C=N), 849 (H_2O), 625 (M–N), 486 (M–O); Anal. Calcd. $C_{46}H_{44}N_8O_9S_2Ni$ (974.96): C 56.62, H 4.55, N 11.49%, Found: C 57.01, H 4.29, N 11.30%.

*2.3.8. Bis(4-benzoyl-3-methyl-1-phenyl-2-pyrazolin-5-one sulfanilamide)diaquacopper(II) Cu(Bmpp-Sn)$_2$(H_2O)$_2$ (**2d**).* Brown solid; yield 92%; mp 238–240°C; Molar cond. (10^{-3} M in DMF): 6.41 ohm^{-1} cm^2 mol^{-1}; μ_{eff} (B.M.): 1.93; UV-Vis (DMF) λ_{max} nm: 273 ($\pi \rightarrow \pi^*$), 378 (n $\rightarrow \pi^*$), 442, 751 (d $\rightarrow$ d); IR KBr (ν_{max}, cm^{-1}): 3498 (N–H), 3399 (O–H), 2935 (C–H), 1617 (C=N), 840 (H_2O), 623 (M–N), 484 (M–O); Anal. Calcd. $C_{46}H_{42}N_8O_8S_2Cu$ (961.80): C 57.39, H 4.40, N 11.65%, Found: C 57.19, H 4.31, N 11.32%.

*2.4. X-Ray Diffraction Study of Bmpp-Sn (**2**).* Single crystal X-ray diffraction studies were performed at 200 K using a Bruker Kappa Apex II diffractometer with graphite monochromator, Mo Kα radiation (λ = 0.71073 Å). APEXII was used for data collection and SAINT for cell refinement and data reduction. The structure was solved by direct methods using SHELXS-97 and refined by least-squares procedures using SHELXL-97 [21] with SHELXLE [22] as a graphical interface. Platon [23] and Ortep-3 [24] were used to prepare material and diagrams, respectively.

2.5. Antibacterial Studies. In vitro antibacterial activity of synthesized compounds was screened against Gram positive *Staphylococcus aureus* and *Bacillus pumilus* and Gram negative *Proteus vulgaris* and *Aeromonas hydrophila* bacterial isolates at 40 mg/mL in DMSO using the Kirby-Bauer disc diffusion technique based on the size of inhibition zone formed around the paper discs with some modifications [25]. Bacterial isolates were grown in freshly prepared nutrient broth growth media to obtain a minimum of 0.1 optical density OD of bacterial isolates suitable for screening. To a solidified about 20 mL Mueller-Hinton agar in Petri plates, 0.1 mL of test bacteria was spread over the medium using a sterilized spreader. Presterilized filter paper discs having a diameter of 6 mm which were impregnated into prepared solutions of synthesized ligands and complexes were placed in the inoculated Petri plates ensuring a reasonable equidistance from each other. Filter paper disc treated with DMSO was used as control while antibacterial chloramphenicol served as a standard drug and was used as a reference to evaluate the potency of the tested compounds under the same conditions. The Petri dishes were left for a few hours in the refrigerator for prediffusion and finally transferred to an incubator at 37°C for 24 h. This procedure was performed in triplicate. The bactericidal activities were determined by measuring the diameter of the zones showing complete inhibition of bacterial growth in millimeters and subtracting the diameter of the filter paper disc and finally dividing by 2 to obtain the exact zone of inhibition. The values were calculated as mean of triplicates.

2.6. Antioxidant (Free Radical Scavenging) Activity. Schiff base free radical scavenging activity and that of its metal complexes were tested against the stable free radical of 1, 1-diphenyl-2-picrylhydrazyl (DPPH), employing the method of Blois [26] with few modifications. A 0.1 mmol solution of the DPPH in methanol was prepared, and 1 mL of this solution was added to 3 mL prepared solutions of the test compounds in a mixture of DMSO and methanol in a mole

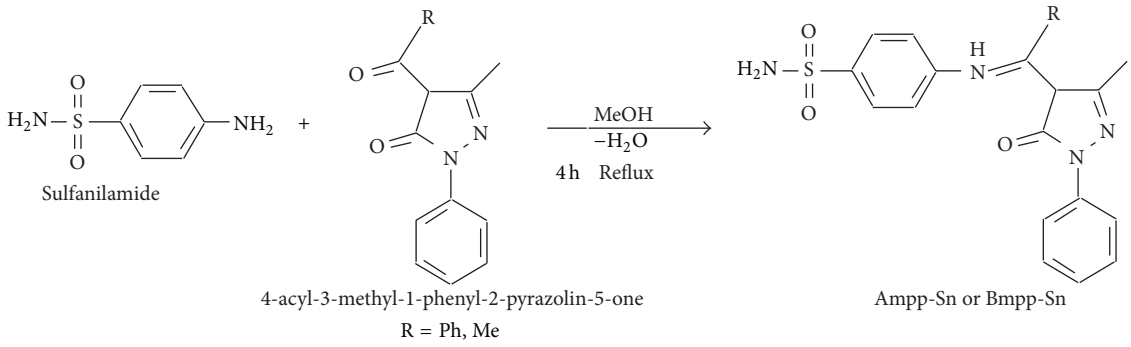

Scheme 1: Synthesis of 4-acyl-3-methyl-1-phenyl-2-pyrazolin-5-one-sulfanilamide.

ratio of 1 : 9, respectively, at different concentrations (0.13, 0.25, and 0.50 mg/mL). The same procedure was carried out for standard drug, ascorbic acid, and an equal volume of dissolving solvents as control. The mixture was shaken vigorously and allowed to stand at room temperature in the dark for 30 min. With the use of a spectrophotometer at a wavelength of 517 nm the absorbance was measured. The capability of synthesized compounds to scavenge DPPH radical was calculated using the expression

$$\text{Scavenging activity (\%)} = \frac{A_0 - A_1}{A_0} \times 100, \quad (1)$$

where A_0 is the absorbance with control sample and A_1 is the absorbance with test samples including that of standard drug.

3. Results and Discussion

3.1. Synthesis. The acylpyrazolone Schiff base precursors, 4-acetyl-3-methyl-1-phenyl-2-pyrazolin-5-one and 4-benzoyl-3-methyl-1-phenyl-2-pyrazolin-5-one, were synthesized using the reported method [20], while the Schiff base ligands 4-acetyl-3-methyl-1-phenyl-2-pyrazolin-5-one sulfanilamide (Ampp-Sn) **1** and 4-benzoyl-3-methyl-1-phenyl-2-pyrazolin-5-one sulfanilamide (Bmpp-Sn) **2** were afforded by the condensation reaction of an aromatic amine 4-aminobenzenesulfonamide (sulfanilamide), with 4-acetyl or 4-benzoyl-3-methyl-1-phenyl-2-pyrazolin-5-one in a 1 : 1 Molar ratio according to the synthetic Scheme 1.

They were obtained in more than 50% yield and recrystallized in methanol. Single threadlike crystal structure of **2** distorted with a water molecule was obtained from slow evaporation of a solution of methanol. Treatment of **1** or **2** with an appropriate metal salt afforded the metal complexes **1a–d** and **2a–d** having a general scheme presented in (2), which shows synthesis of 4-acyl-3-methyl-1-phenyl-2-pyrazolin-5-one-sulfanilamide transition metal complexes. Their Molar conductance values infer a nonelectrolyte behavior in DMF [27]:

$$\mathrm{MX_2 \cdot \mathit{n}H_2O} \xrightarrow[\text{reflux,4 h}]{\mathrm{EtOH/H_2O}} \mathrm{ML_2\left(H_2O\right)_2 \cdot \mathit{n}H_2O} \quad (2)$$

$$\mathrm{M = Mn^{2+}\,(\mathbf{a}),\ Co^{2+}\,(\mathbf{b}),\ Ni^{2+}\,(\mathbf{c}),\ Cu^{2+}\,(\mathbf{d});\ X = Cl^{-}\ or\ CH_3COO^{-};\ L = Ampp\text{-}Sn\,(\mathbf{1})\ or\ Bmpp\text{-}Sn\,(\mathbf{2}).}$$

The elemental percentage composition of **1**, **2**, **1a–d,** and **2a–d** found was in agreement with calculated values. Octahedral metal complexes with the corresponding Schiff base binding bidentately are proposed, having two molecules each of the Schiff base and two molecules of water to complete its octahedral geometry [28].

3.2. ^1H and ^{13}C NMR Spectroscopy. The ^{1}H NMR spectra of **2** showed a multiplet at 7.8–7.1 ppm due to the aromatic protons and a singlet each at 12.8 ppm and at 8.0 ppm, Figure 1, assigned, respectively, to the sulfanilamide NH_2 hydrogen –NH and the azomethine nitrogen H–N=C proton. The resonance peak due to methyl protons on the pyrazolone ring is displayed upfield at 2.2 ppm integrating for an unequivalent number of hydrogen atoms.

^{1}H NMR spectrum of **1** was inconclusive as resonance peaks were not resolved enough to assign all necessary chemical shifts; however, the peak on the far downfield is due to sulfanilamide NH_2 hydrogen –NH at 13.1 ppm integrated for one proton. The two sharp peaks observed at the far upfield are due to the methyl proton groups, pyrazolone methyl at 2.5 ppm, and the acetyl methyl at 2.4 ppm, although integrated for a higher proton value. The signals at 7.9–7.2 ppm are assigned to the aromatic protons while the peak at 8.0 ppm is due to azomethine hydrogen H–N=C, Figure 2.

The ^{13}C NMR spectra gave more information on the Schiff base ligands, Figures 3 and 4. A signal at 190.5 ppm in

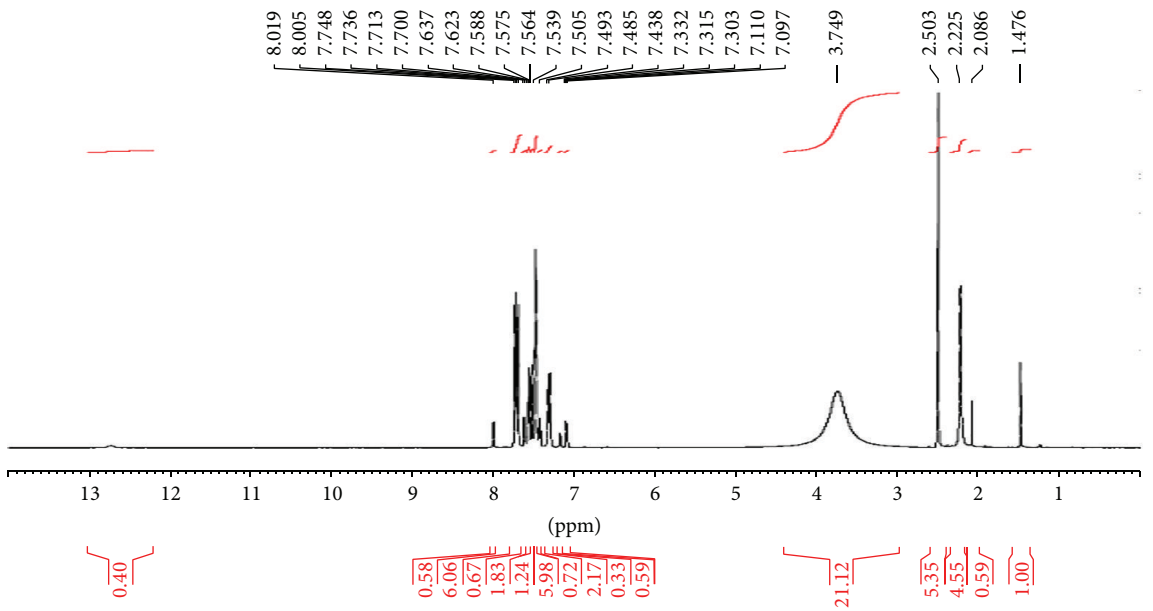

Figure 1: ^{1}H NMR spectrum of Bmpp-Sn (**2**).

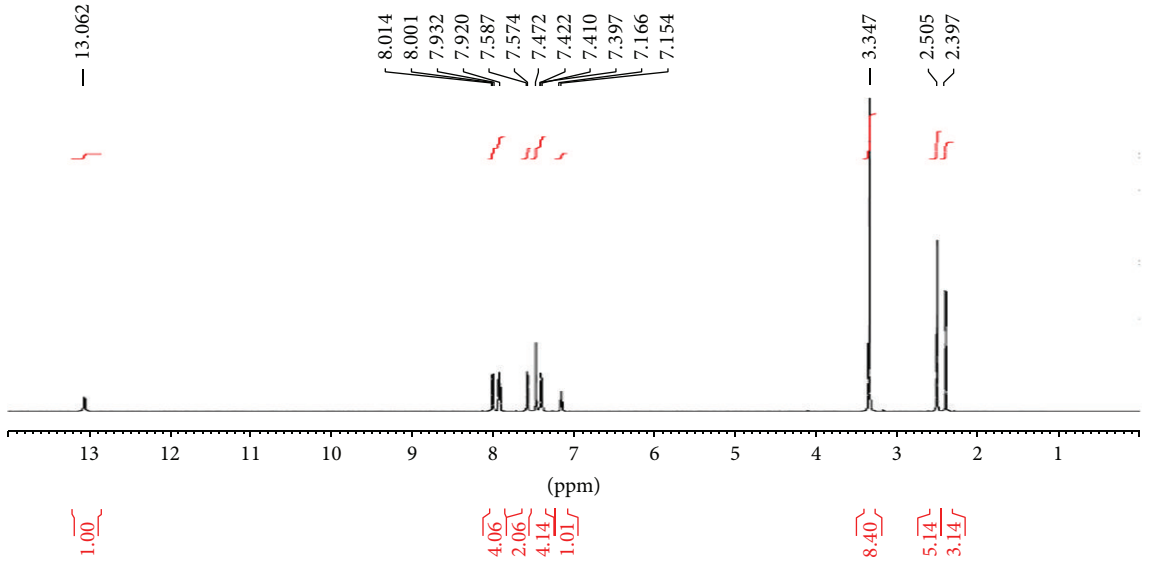

Figure 2: ^{1}H NMR spectrum of Ampp-Sn (**1**).

2 and that at 165.4 ppm in **1** may be assigned to the carbonyl carbon C=O. The azomethine carbon is observed at 139.3 ppm in the spectrum of **2** and at 164.5 ppm in **1** [29]. Signals due to aromatic carbon atoms are resonating at a chemical shift of 132.2–110.7 ppm in **2** and 142.8–116.6 ppm in **1**. Aliphatic methyl carbon may be assigned to a signal at around 16.5 ppm in **2** and the two methyl groups in **1** are assigned to the signals at 17.6 and 17.5 ppm.

The resonance signal due to C–S may be assigned to the signal at 148.2 ppm in **1**. Unfortunately, this particular signal could not be accounted for in **4** but its mass spectrum and crystal X-ray structure do confirm the proposed molecular structure.

3.3. Mass Spectroscopy. The molecular ion peak of the APCI source mass spectrum of **2** and **1** was observed at *m*/*z* 433 and *m*/*z* 371, respectively, and in agreement with the calculated theoretical Molar mass plus one hydrogen $[M + H]^{+}$, equivalent protonated ligands, Figures 5 and 6.

Also the protonated benzoyl Schiff base precursor fragmentation peak was observed at *m*/*z* 279, that is, $C_{17}H_{14}N_2O_2$ in **2**, while that of acetyl Schiff base precursor $C_{12}H_{11}N_2O_2$ was seen at *m*/*z* 216 in the spectrum of **1**.

3.4. FT-IR Spectroscopy. The successful coordination of the sulfanilamide with acylpyrazolone to form the keto-imine tautomer Schiff bases was evident in the presence of

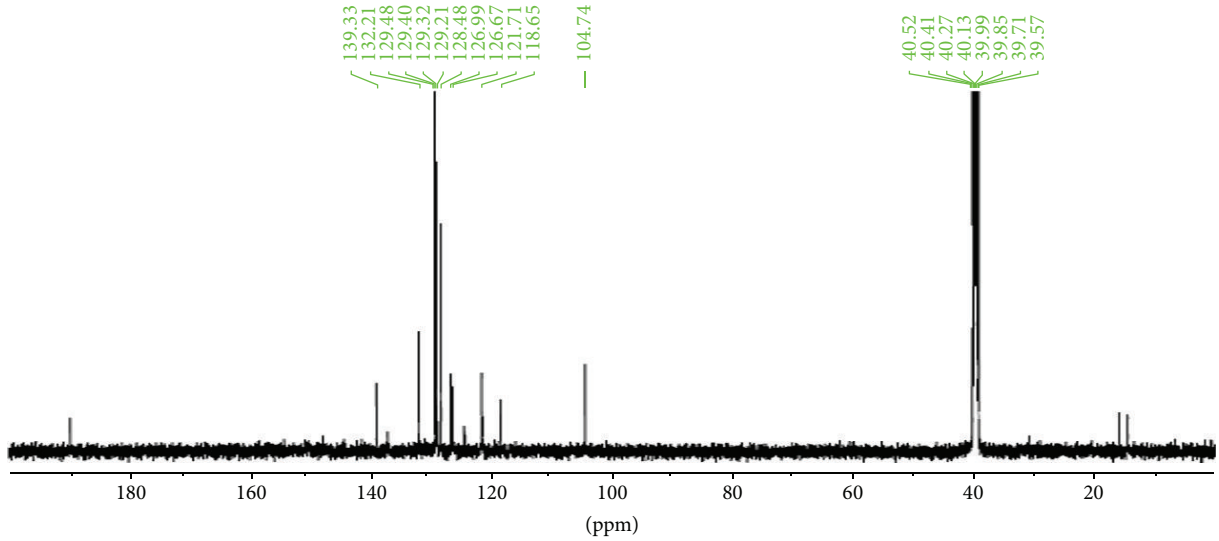

Figure 3: ^{13}C NMR spectrum of Bmpp-Sn (**2**).

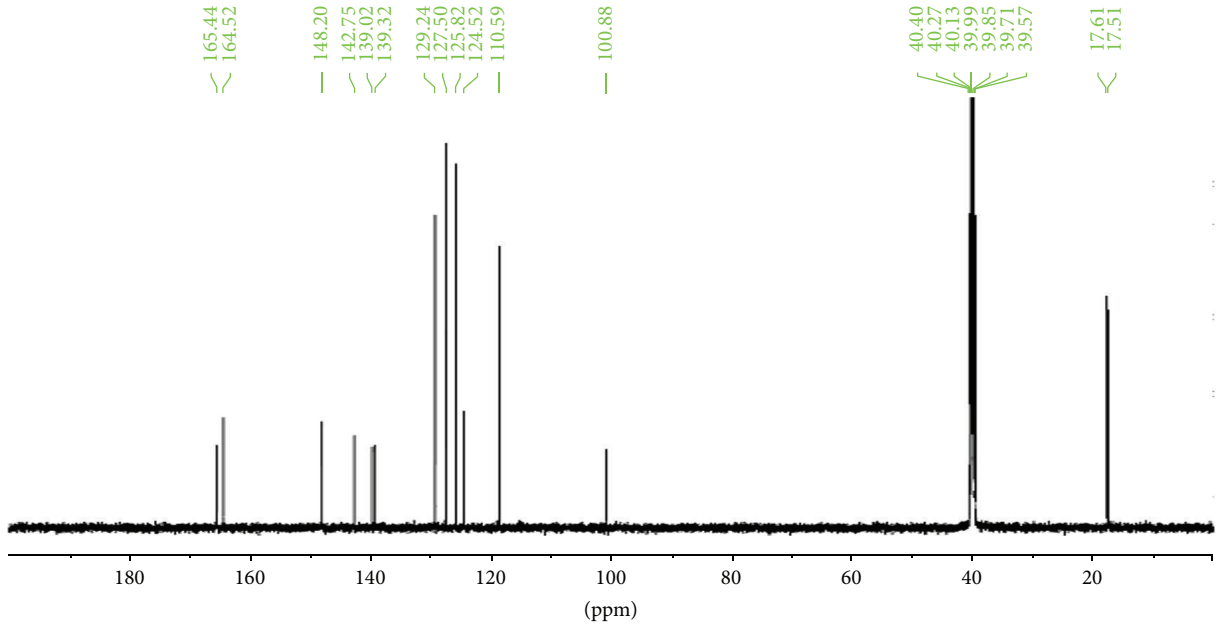

Figure 4: ^{13}C NMR spectrum of Ampp-Sn (**1**).

the azomethine (C=N) and ketone carbonyl (C=O) vibrating bands in their IR spectra. The (C=N) was observed at 1639 cm^{-1} in **2** and 1633 cm^{-1} in **1** which was modified and appeared at a lower wave number region of 1627–1617 cm^{-1} in the IR spectra of the metal complexes [30]. Ketone carbonyl group (C=O) was prominently observed at 1504 cm^{-1} in **2** and 1503 cm^{-1} in **1**, which were reduced in peak size or have disappeared in their corresponding metal complexes spectra showing a transformation of the double bond of carbonyl into a metal oxygen bond –C–O–M [31]. The octahedral Schiff base metal complexes were completed with two water molecules each and this bond can be seen from the formation of a vibrating band at around 850–823 cm^{-1} in addition to the broad band at 3498–3390 cm^{-1} due to the –OH from the water molecules, which appeared originally at 3496–3497 cm^{-1} in **1** and **2** due to the –NH and –OH stretching frequencies [32]. The stretching bands that appeared at 634–619 cm^{-1} and 498–470 cm^{-1} are due to metal nitrogen bond M–N and that of metal oxygen M–O, respectively [33].

3.5. UV-Visible Spectroscopy and Magnetic Moment. Bmpp-Sn and Ampp-Sn exhibited bands at the UV region due to charge transfer $\pi \rightarrow \pi^*$ and n $\rightarrow \pi^*$ transitions, which are usually intense as a result of the organic conjugate π bonds of the benzene ring [34]. Charge transfer transitions may interfere with each other, therefore preventing the expected

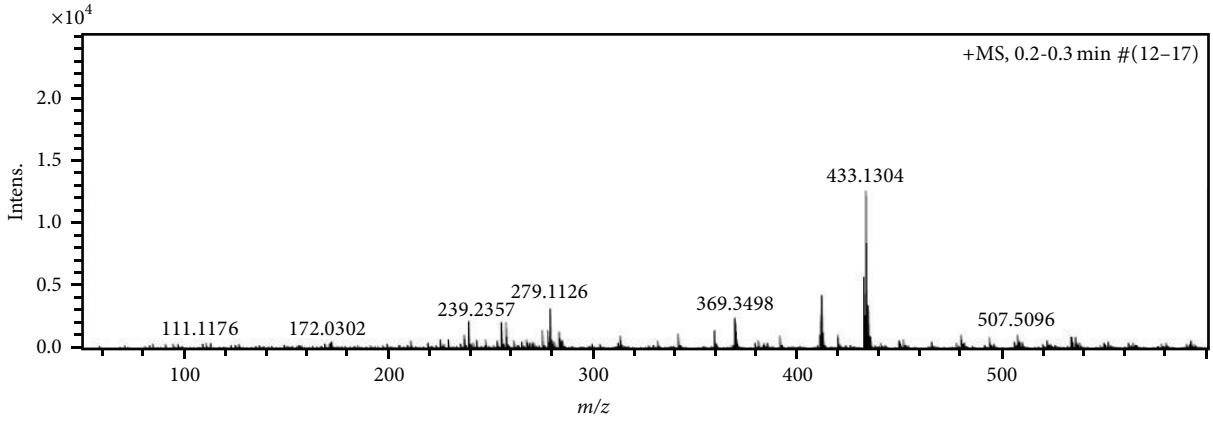

Figure 5: Mass spectrum of Bmpp-Sn (**2**).

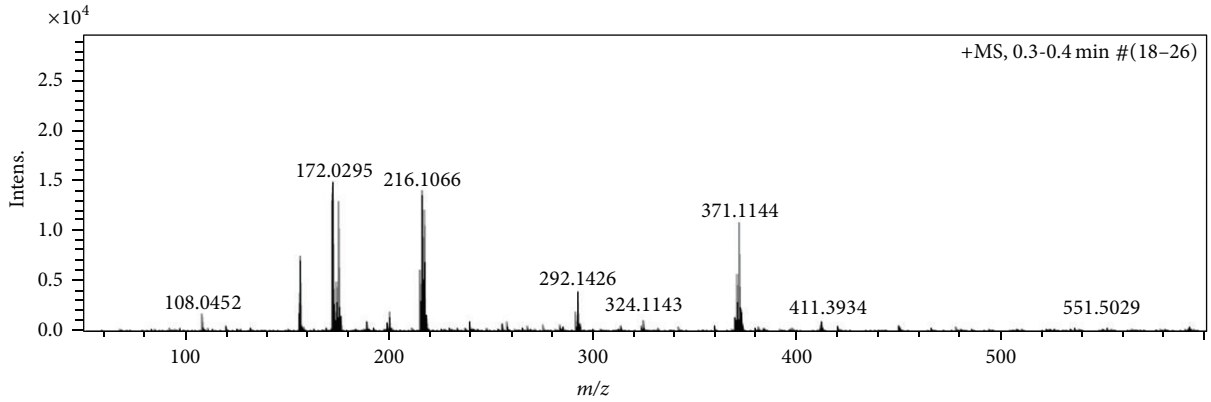

Figure 6: Mass spectrum of Ampp-Sn (**1**).

transitions in the visible region of the electronic spectra of compounds to be observed, as seen in the spectra of some of the metal complexes reported herein [35]. Absorption bands and wavelength values carefully assigned are presented in the experimental section. **2a** shows two bands in the visible region at 424 nm and 589 nm assigned to $^6A_{1g} \rightarrow {}^4T_{2g}$ and $^6A_{1g} \rightarrow {}^4T_{1g}$ transitions, respectively, corresponding to a d^5 octahedral Mn(II) complex [36]. One band at 431 nm is assigned to $^6A_{1g} \rightarrow {}^4T_{2g}$ in **1a**. The high spin d^5 octahedral manganese complexes were corroborated with the magnetic moment values of 5.82 and 5.61 BM for **2a** and **1a,** respectively [37]. **2b** displays two bands in the visible region at 408 nm and 540 nm corresponding to ν_1 ($^4T_{2g} \rightarrow {}^4T_{1g}$) and ($^4A_{2g} \rightarrow {}^4T_{1g}$) transitions, respectively. It similarly has a magnetic moment value of 4.46 BM, expected for an octahedral Co(II). Three bands were observed in the electronic spectra of **1b** with magnetic moment of 4.43 BM, at 408 nm, 632 nm, and 699 nm assigned as ($^4T_{2g} \rightarrow {}^4T_{1g}$), ($^4A_{2g} \rightarrow {}^4T_{1g}$), and ($^4T_{1g(p)} \rightarrow {}^4T_{1g}$) transitions, respectively, peculiar to a d^7 octahedral geometry [38] (Figure 7).

The absorption bands at 410 nm and 683 nm were assigned to $^3A_{2g} \rightarrow {}^3T_{1g(p)}$ and $^3A_{2g} \rightarrow {}^3T_{1g(F)}$, respectively, in **2c**. In **1c** the d-d bands at 596 nm and 674 nm are assigned

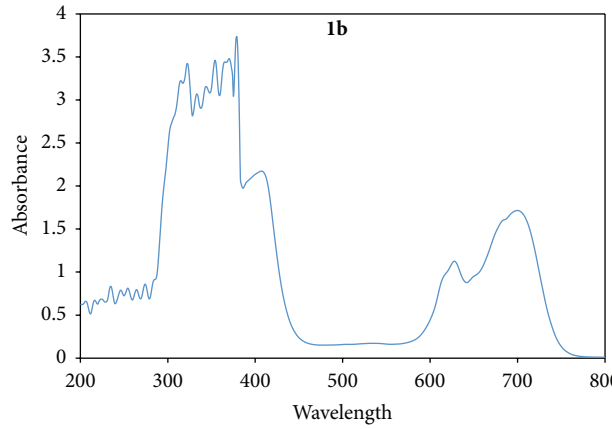

Figure 7: Electronic spectrum of $Co(Ampp\text{-}Sn)_2(H_2O)_2$ (**1b**).

to $^3A_{2g} \rightarrow {}^3T_{1g(F)}$ and $^3A_{2g} \rightarrow {}^3T_{2g(F)}$ transitions, respectively. These transitions correspond to a d^8 Ni(II) with octahedral geometry. Their magnetic moment of 2.89 and 2.93 BM for **2c** and **1c**, respectively, further justifies the proposed geometries [39]. Two bands in the electronic spectra of **2d**, observed as a strong band at 442 nm and a broad band that

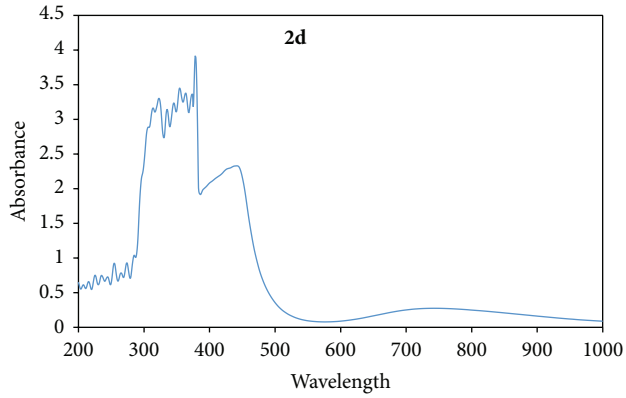

FIGURE 8: Electronic spectrum of $Cu(Bmpp\text{-}Sn)_2(H_2O)_2$ (**2d**).

peaks at 751 nm, were assigned to $^2B_{1g} \rightarrow {}^2E_g$ and $^2B_{1g} \rightarrow {}^2B_{2g}$ transitions, respectively (Figure 8), with a magnetic moment value of 1.93 BM. **1d** exhibited one single broad band characterized by a distorted octahedral Cu(II) at 618 nm which is assigned to $^2B_{1g} \rightarrow {}^2B_{2g}$ transition, with a magnetic moment value of 1.90 BM [38].

3.6. Thermogravimetric Analysis. TGA in collaboration with DTG results shows a multistep decomposition pattern in the thermograms of some of the metal complexes under investigation. Generally, relatively low thermal decomposition mass losses observed below 300°C are due to the removal of the coordinated and noncoordinated water molecules, although not so in some of the metal complexes with coordinated water molecule [40]. As they exhibited multiple decomposition steps, their assignments were not unequivocal. In **2a** the decomposition due to the removal of the four water molecules is observed at 220°C. The major decomposition at around 550°C with a mass loss of about 44% may be attributed to the removal of a molecule of **2** calculated as 45.3%. This decomposition was followed by a second, over a wide temperature range extending beyond 900°C, which may be attributed to the second Schiff base ligand, leaving a residue of manganese oxide. Schiff base ligands with more aromatic groups are generally more stable; hence the varying trends of decomposition are shown by **1a**–**d** as we proceed. The decomposition due to the elimination of the water molecules in **1a** is observed at 150 and 290°C. It was followed by a major decomposition at around 450°C attributed to the decomposition of a molecule of **1** with a mass loss of 40% and calculated as 43.7%. The final decomposition due to the second ligand extends beyond 900°C leaving the metal oxide. The removal of water molecules from **4b** was observed at around 100°C. The major decomposition at 400°C was attributed to the loss of **4** with a mass percentage of 45% which was calculated as 44.3%. The third decomposition over a wide temperature range was attributed to the second Schiff base ligand leaving a cobalt oxide residue behind with a percentage mass of 6.9% and calculated as 7.7% (Figure 9). The thermogram for **1b** exhibited multiple decompositions bringing about unequivocal assignments an evidence of its low thermal stability. However, the water molecules elimination can be observed at 160°C.

Complex **2c** (Figure 10) exhibited decompositions due to water molecules at around 80 and 140°C. Its major decomposition occurred at 420°C associated with the removal of a molecule of **2** with an equivalent mass loss of 50% and calculated as 50.9%. The final decomposition at around 810°C was attributed to the removal of a total of four molecules of water and two molecules of the Schiff base leaving behind a nickel oxide residue with a percentage mass of 9% and calculated as 8.7%.

Another multistep decomposition trend was observed in **1c**. The elimination of the water molecules was evident from the decompositions at 170 and 280°C. A major decomposition due to the removal of a **1** molecule was observed at 440°C with a mass loss of 44% which is in agreement with the calculated mass loss of 43.5%. The final decomposition due to the removal of the second Schiff base extends beyond 900°C which was terminated with the left over nickel oxide. The thermal decomposition of **2d** showed an unexpected one decomposition step at 330°C which cannot be easily assigned. This observation may be due to the formation of gaseous reaction products. Also unexpectedly, the coordinated water molecule in **1d** cannot be accounted for in the TGA curve but a major decomposition at 440°C may be due to the elimination of one Schiff base ligand with a mass loss of 45%, calculated as 43.2% (Figure 11). This was followed by a second and final decomposition attributed to the fragmentation of the last **1** molecule, leaving behind a residue of the metal oxide with a remaining mass of around 11%, calculated as 8.8%.

On the basis of elemental analysis and spectroscopic and TGA results the proposed structures of metal complexes may be represented as seen in Figure 12.

3.7. Crystallographic Data. Slow evaporation of **2** in methanol afforded needle-like single crystals of Schiff base **2** with a water molecule distortion formulated as $C_{23}H_{20}N_4O_3S{\cdot}H_2O$. A summary of crystal data is presented in Table 1.

Solid state molecular structure of $Bmpp\text{-}Sn{\cdot}H_2O$ as seen in Figure 13 is essentially planar with the plane of the methylpyrazolone group but with the phenyl groups turned out of the plane in accordance with reported crystal structures [18, 28]. The phenyl rings C11–C16, C21–C26, and C31–C36 make dihedral angles of 39.44(12)°, 66.26(13)°, and 34.38(13)°, respectively, with the methylpyrazolone group.

There are three intramolecular bonds: one short N2···H2···O3 hydrogen bond of 1.90 Å and two long C13···H13···O2 and C32···H32···O3 hydrogen bonds of 2.48 Å each (Figure 14).

Pairs of $Bmpp\text{-}Sn{\cdot}H_2O$ are alternatively stacked in the c-axis direction and connected with two C22···H22···O3 hydrogen bonds of 2.45 Å, two C16···H16···C (pyrazole ring) π-ring interactions of 2.66 Å, and two N1···H1B···C (C31–C36 phenyl ring) π-ring interaction of 2.70 Å. A water molecule connects adjacent $Bmpp\text{-}Sn{\cdot}H_2O$ in the b-axis direction with two hydrogen bonds N1···H1A···O4···H4B···N4 of length 1.74 and 2.13 Å, respectively. Crystallographic data for the structural analysis have been deposited

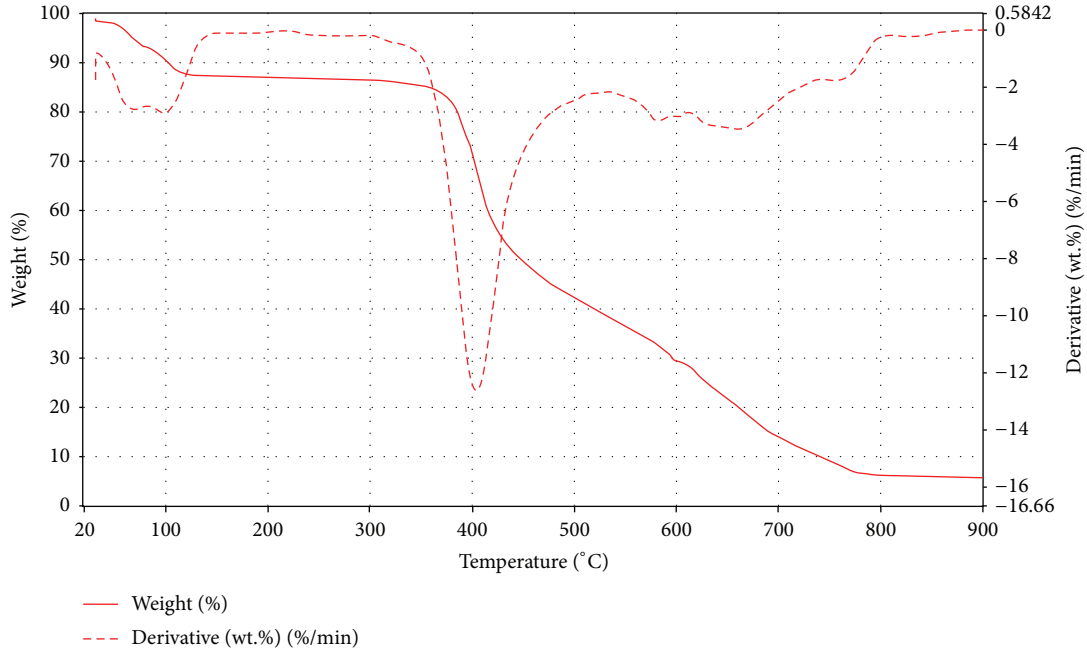

Figure 9: TGA and DTG curve of $Co(Bmpp\text{-}Sn)_2(H_2O)_2{\cdot}H_2O$ (**2b**).

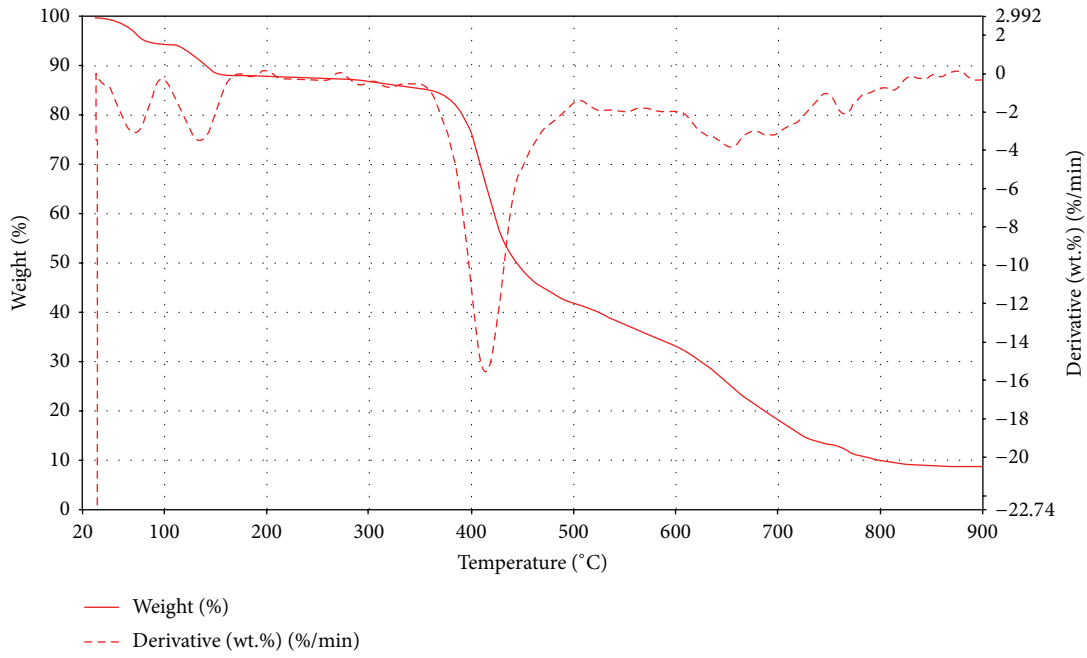

Figure 10: TGA and DTG curve of $Ni(Bmpp\text{-}Sn)_2(H_2O)_2{\cdot}H_2O$ (**2c**).

with the Cambridge Crystallographic Data Centre, CCDC, number 923953.

3.8. Antibacterial Activity. A generally moderate to poor activity of reported compounds with some showing no activity at all is observed relative to the standard chloramphenicol drug, as seen from the mean values of bacterial growth inhibition zones carried out in triplicate at 40 mg/mL concentration. **2** exhibited a broad spectrum activity (active against all selected bacterial isolates) and showed the highest zone of inhibition value of 24 mm against *Aeromonas hydrophila* (Table 2). **2b**, **2c**, **1c**, and **1** on the other hand exhibited activity against three of the selected bacterial isolates.

Although it is expected that chelation of metal ion to Schiff base does increase the possibility of microbial growth

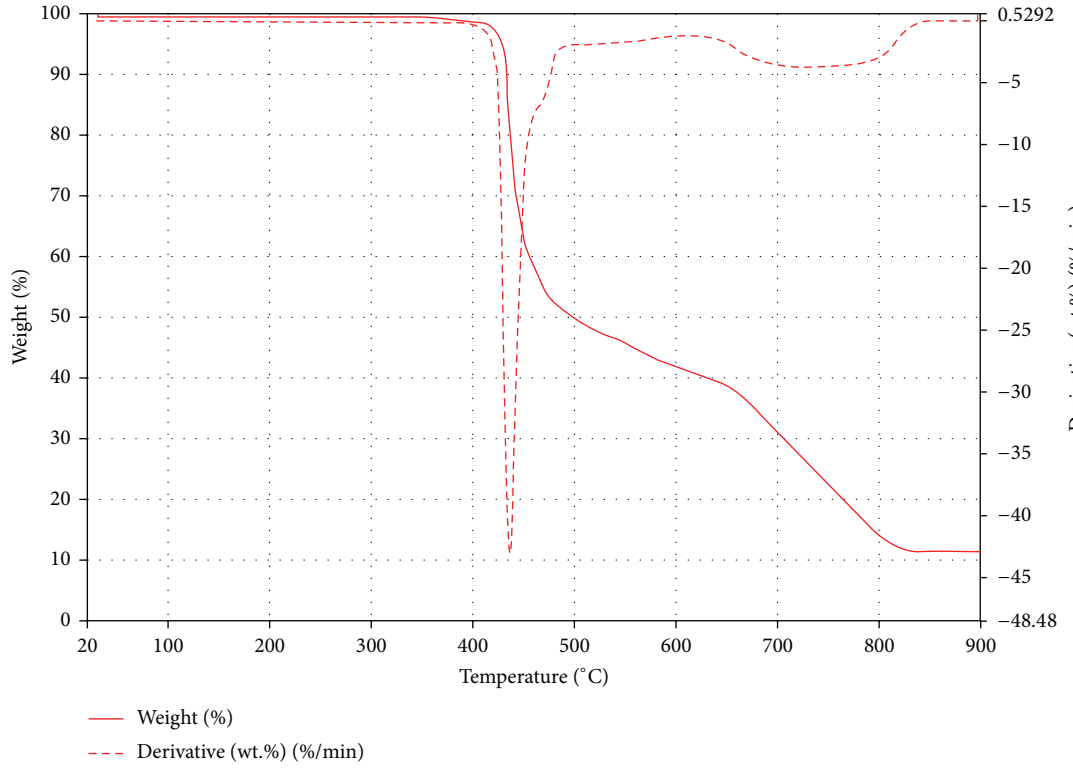

Figure 11: TGA and DTG curve of $Cu(Ampp\text{-}Sn)_2(H_2O)_2{\cdot}H_2O$ (**1d**).

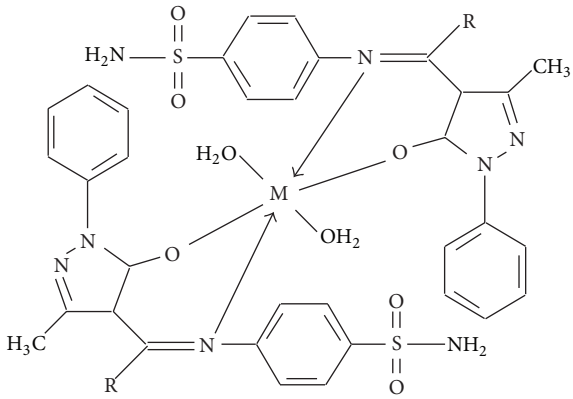

Figure 12: Proposed structural scheme for metal complexes.

Table 1: Crystal data for **2**.

Compound	Bmpp-Sn
Formula	$C_{23}H_{20}N_4O_3S{\cdot}H_2O$
Crystal colour and form	Orange/block
Formula weight	450.52
Crystal system	Monoclinic
Space group	C2/c
a	23.3366 (4) (Å)
b	14.7706 (3) (Å)
c	12.5787 (2) (Å)
α	90 (2)°
β	100.727 (2)°
V	4257.21 (13) ($Å^3$)
Z	8
$D_{(calc)}$	1.406 ($Mg\,cm^{-1}$)
$F(000)$	1888
θ range	2.2–28.3 (°)
Crystal size	0.24 × 0.38 × 0.56 (mm)
Reflections measured	19945
Independent/observed	5285/4408
Mu(MoKa)	0.71073 (/mm)
Temperature	296 (K)
Parameters	108

inhibition [41], the observed variation herein may be as a result of impermeability of bacterial isolates cell wall or the nature of their ribosomes [42].

3.9. Antioxidant (Free Radical Scavenging) Activity. The reduction/scavenging capability is taken as the decrease in absorbance at a constant wavelength relative to the control sample which is made possible by antioxidant properties [43]. It is evident that the potential antioxidant properties of some naturally occurring ingredients from plants and synthetic analogs are as a result of having electron-donating groups [44] and as such the inductive effects of the sulfur and

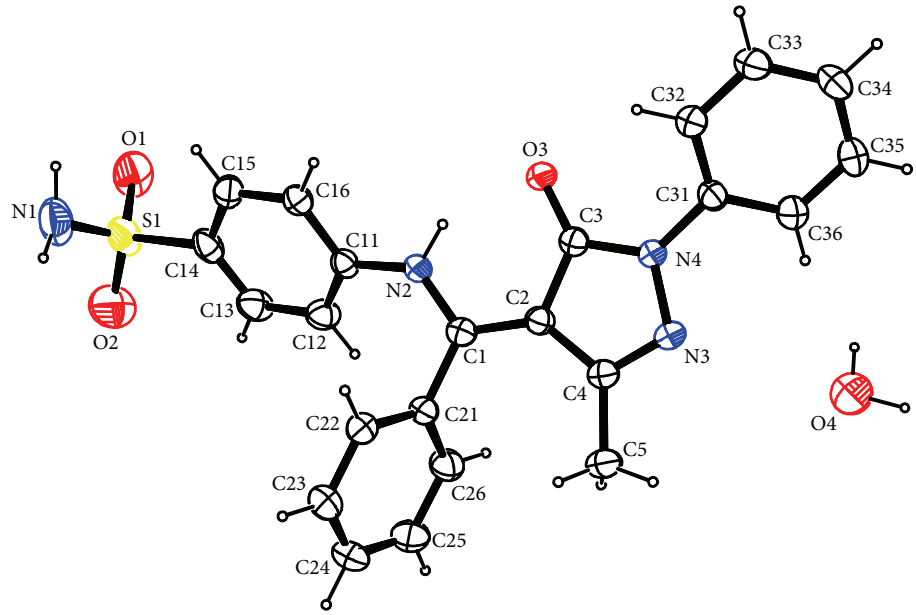

Figure 13: Molecular crystal structure of Bmpp-Sn·H_2O.

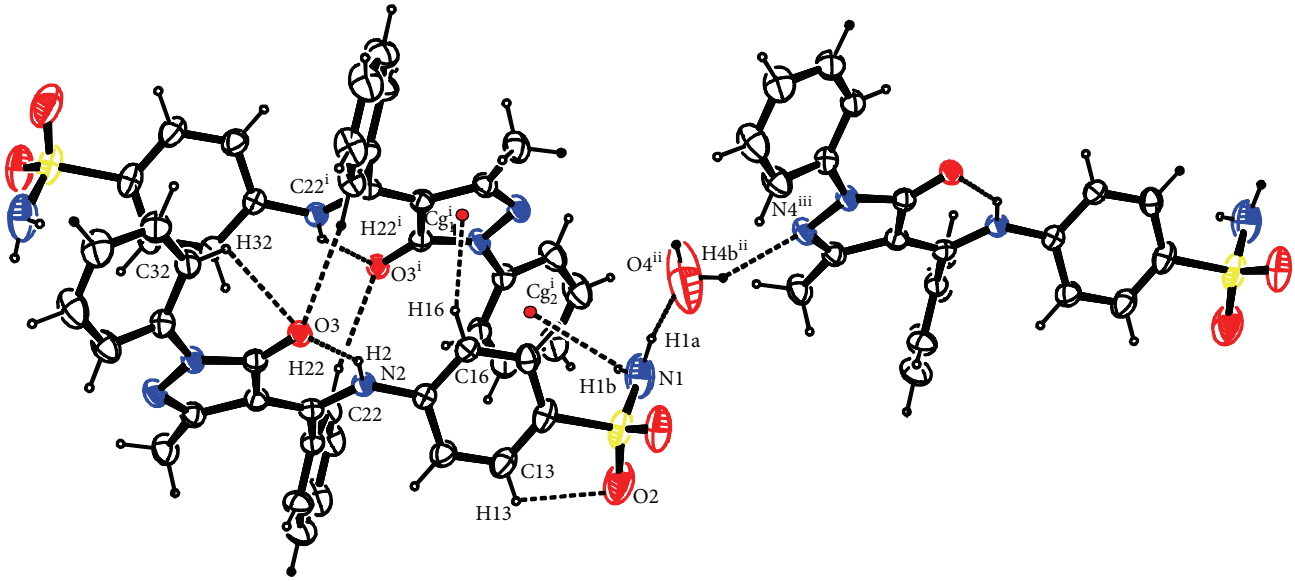

Figure 14: Hydrogen bonding in Bmpp-Sn·H_2O.

nitrogen groups in **1** and **2** may be able to push electron density towards the free radicals to produce relatively stable molecules. The metal complexes exhibited a generally low antioxidant property compared to standard drug ascorbic acid (Figure 15). However, **1c** showed very strong antioxidant activities having values almost equal to that of ascorbic acid in all three different concentrations. **1a** as well as **1b** exhibited strong antioxidant properties higher than their Schiff base ligand **1,** which is in agreement with previously reported compounds coordinated to transition metal ions [45].

On comparing the metal complexes with their corresponding ligands, **2** showed a stronger free radical scavenging property at all three different concentrations contrary to **1**.

4. Conclusions

The reported results herein support the successful synthesis of new possible therapeutic Schiff bases and their metal complexes. A keto-imine tautomer of **1** and **2** has been established with good bioactivity, more of which were free radicals scavengers (antioxidant activity). Single crystal X-ray analysis further confirms the structure of **2** and an octahedral geometry of metal complexes with two molecules of Schiff base ligand and H_2O molecule each have been proposed by way of analytical and spectroscopic techniques. A good number of the synthesized compounds have been identified as potential bactericidals and putting their antioxidant activities

Table 2: Zone of growth inhibition exhibited by sulfanilamide Schiff bases and metal complexes at 40 mg/mL (mm).

Ligand and complexes	*Staphylococcus aureus*	*Bacillus pumilus*	*Proteus vulgaris*	*Aeromonas hydrophila*
2	12.5	7.5	10.3	24.0
1	NI	5.0	8.5	4.0
2a	8.5	NI	NI	8.0
2b	13.3	16.0	NI	15.0
2c	8.0	NI	11.5	21.0
2d	NI	10.3	NI	8.0
1a	NI	NI	NI	8.5
1b	NI	9.0	NI	NI
1c	4.5	6.0	NI	6.0
1d	NI	NI	8.5	15.0
Chloramphenicol	30.0	20.0	42.0	40.0
DMSO	NI	NI	NI	NI

NI = no inhibition.

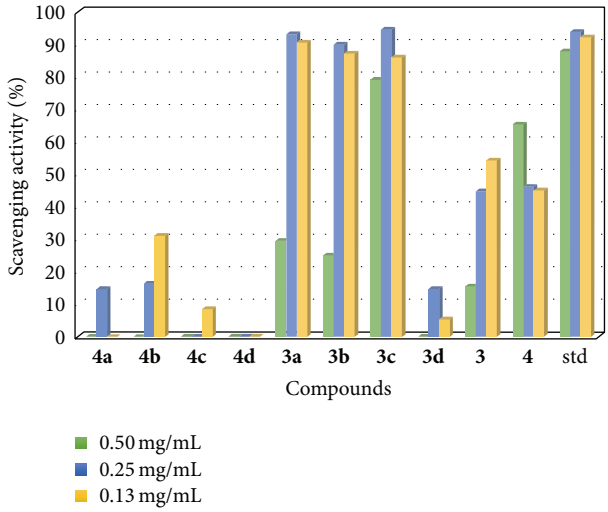

Figure 15: Chart showing the scavenging activity.

into consideration, synthesized compounds may be useful antitumour candidates.

Additional Information

Crystallographic data for 4-benzoyl-3-methyl-1-phenyl-2-pyrazolin-5-one sulfanilamide reported herein has been deposited with the Cambridge Crystallographic Data Centre (CCDC) number 923953. Copies of this information may be obtained free of charge from the Director, CCDC, 12 Union Road, Cambridge CB2 1EZ [Fax: +44 1223 336 033], or deposit@ccdc.cam.ac.uk or http://www.ccdc.cam.ac.uk.

Conflict of Interests

The authors declare that there is no conflict of interests regarding the publication of this paper.

Acknowledgments

The financial support of the Govan Mbeki Research and Development Centre (GMRDC), University of Fort Hare, and National Research Foundation (NRF)/Sasol Inzalo Foundation (SIF) is appreciated. Omoruyi G. Idemudia thank the NRF/SIF for the award of a PDF (Grant UID: 92275).

References

[1] A. Iqbal, H. L. Siddiqui, C. M. Ashraf, M. H. Bukhari, and C. M. Akram, "Synthesis, spectroscopic and cytotoxic studies of biologically active new Schiff bases derived from p-nitrobenzaldehyde," *Chemical and Pharmaceutical Bulletin*, vol. 55, no. 7, pp. 1070–1072, 2007.

[2] M. Singh and N. Raghav, "Biological activities of hydrazones: a review," *International Journal of Pharmacy and Pharmaceutical Sciences*, vol. 3, no. 4, pp. 26–32, 2011.

[3] A. Rezaeifard, M. Jafarpour, M. A. Nasseri, and R. Haddad, "Pronounced catalytic activity of manganese(III)—schiff base complexes in the oxidation of alcohols by tetrabutylammonium peroxomonosulfate," *Helvetica Chimica Acta*, vol. 93, no. 4, pp. 711–717, 2010.

[4] J. T. Su, P. Vachal, and E. N. Jacobsen, "Practical synthesis of a soluble schiff base catalyst for the asymmetric strecker reaction," *Advanced Synthesis and Catalysis*, vol. 343, no. 2, pp. 197–200, 2001.

[5] A. K. Singh and M. A. Quraishi, "Study of some bidentate schiff bases of isatin as corrosion inhibitors for mild steel in hydrochloric acid solution," *International Journal of Electrochemical Science*, vol. 7, no. 4, pp. 3222–3241, 2012.

[6] H. Ju, Z.-P. Kai, and Y. Li, "Aminic nitrogen-bearing polydentate Schiff base compounds as corrosion inhibitors for iron in acidic media: a quantum chemical calculation," *Corrosion Science*, vol. 50, no. 3, pp. 865–871, 2008.

[7] P. Butvin, S. Lubkeova, K. Capalova, and Z. Pikulikova, "Liquid extraction of copper(ll) and some bivalent metal ions by salicylidenalkylimines and A/-(2-hydroxybenzyl)alkylamines," *Chemical Papers*, vol. 48, no. 1, pp. 15–20, 1994.

[8] Z. Shiri-Yekta and M. R. Yaftian, "Anion control selectivity of neutral N4-type schiff base extractants towards transition metal ions," *Iranian Journal of Chemistry and Chemical Engineering*, vol. 29, no. 2, pp. 11–17, 2010.

[9] O. G. Idemudia and E. C. Hosten, "Bis(4-benzoyl-3-methyl-1-phenyl-1*H*-pyrazol-5-olato-$\kappa^2 O,O'$)bis(ethanol-κO)cobalt(II)," *Acta Crystallographica E: Structure Reports Online*, vol. 68, part 8, pp. m1107–m1108, 2012.

[10] F. Marchetti, C. Pettinari, and R. Pettinari, "Acylpyrazolone ligands: synthesis, structures, metal coordination chemistry and applications," *Coordination Chemistry Reviews*, vol. 249, no. 24, pp. 2909–2945, 2005.

[11] N. D. Ekekwe, A. J. Arinze, L. A. Nnanna, C. F. Ukpabi, A. Agwu, and M. O.C. Ogwuegbu, "Synthesis, complexation and characterization of 1-phenyl-3-Methyl-4- (p-nitrobenzoyl) pyrazolone-5(HNPz) and its complexes of barium(II), strontium(II) and zinc(II)," *The American Journal of Chemistry*, vol. 2, no. 2, pp. 52–56, 2012.

[12] H. Zhang, J. Li, Y. Zhang, D. Zhang, and Z. Su, "4-[(*Z*)-(*n*-Butylamino)(2-furyl)methylene]-3-methyl-1-phenyl-1H-pyrazol-5(4*H*)-one," *Acta Crystallographica Section E Structure Reports Online*, vol. 63, no. 8, pp. o3536–o3536, 2007.

[13] G. Mariappan, B. P. Saha, L. Sutharson, G. Ankits, L. Pandey, and D. Kumar, "Evaluation of antioxidant potential of pyrazolone derivatives," *Journal of Pharmacy Research*, vol. 3, no. 12, pp. 2856–2859, 2010.

[14] R. R. Coombs, M. K. Ringer, J. M. Blacquiere et al., "Palladium(II) Schiff base complexes derived from sulfanilamides and aminobenzothiazoles," *Transition Metal Chemistry*, vol. 30, no. 4, pp. 411–418, 2005.

[15] M. Das and S. E. Livingstone, "Cytotoxic action of some transition metal chelates of Schiff bases derived from S-methyldithiocarbazate," *British Journal of Cancer*, vol. 37, no. 3, pp. 466–469, 1978.

[16] M. A. Ali, A. H. Mirza, R. J. Butcher, M. T. H. Tarafder, T. B. Keat, and A. M. Ali, "Biological activity of palladium(II) and platinum(II) complexes of the acetone Schiff bases of S-methyl- and S-benzyldithiocarbazate and the X-ray crystal structure of the [Pd(asme)2] (asme=anionic form of the acetone Schiff base of S-methyldithiocarbazate) complex," *Journal of Inorganic Biochemistry*, vol. 92, no. 3-4, pp. 141–148, 2002.

[17] Y.-Z. Tang, H.-R. Wen, J. Zhang, and Y.-H. Tan, "Synthesis, crystal structure and fluorescent property of a new sulfanilamide schiff-base compound," *Chinese Journal of Structural Chemistry*, vol. 29, no. 1, pp. 69–73, 2010.

[18] O. G. Idemudia, A. P. Sadimenko, A. J. Afolayan, and E. C. Hosten, "3-Methyl-1-phenyl-4-[(phenyl)(2-phenyl-hydrazin-1-yl)methylidene]-1H-pyrazol-5(4H)-one," *Acta Crystallographica Section E: Structure Reports Online*, vol. 68, no. 5, pp. o1280–o1281, 2012.

[19] O. G. Idemudia, A. P. Sadimenko, and E. C. Hosten, "4-{[2-(2,4-Dinitrophenyl) hydrazinylidene] (phenyl)methyl}-5-methyl-2-phenyl-1H-pyrazol-3(2H)-one ethanol monosolvate," *Acta Crystallographica*, vol. E68, p. o3380, 2012.

[20] S. Parihar, S. Pathan, R. N. Jadeja, A. Patel, and V. K. Gupta, "Synthesis and crystal structure of an oxovanadium(IV) complex with a pyrazolone ligand and its use as a heterogeneous catalyst for the oxidation of styrene under mild conditions," *Inorganic Chemistry*, vol. 51, no. 2, pp. 1152–1161, 2012.

[21] G. M. Sheldrick, "A short history of *SHELX*," *Acta Crystallographica Section A: Foundations of Crystallography*, vol. 64, no. 1, pp. 112–122, 2007.

[22] C. B. Hübschle, G. M. Sheldrick, and B. Dittrich, "*ShelXle*: a Qt graphical user interface for SHELXL," *Journal of Applied Crystallography*, vol. 44, no. 6, pp. 1281–1284, 2011.

[23] A. L. Spek, "Single-crystal structure validation with the program PLATON," *Journal of Applied Crystallography*, vol. 36, no. 1, pp. 7–13, 2003.

[24] C. F. Macrae, I. J. Bruno, J. A. Chisholm et al., "Mercury CSD 2.0—new features for the visualization and investigation of crystal structures," *Journal of Applied Crystallography*, vol. 41, no. 2, pp. 466–470, 2008.

[25] A. W. Bauer, W. M. Kirby, J. C. Sherris, and M. Turck, "Antibiotic susceptibility testing by a standardized single disk method.," *The American Journal of Clinical Pathology*, vol. 45, no. 4, pp. 493–496, 1966.

[26] M. S. Blois, "Antioxidant determinations by the use of a stable free radical," *Nature*, vol. 181, no. 4617, pp. 1199–1200, 1958.

[27] W. J. Geary, "The use of conductivity measurements in organic solvents for the characterisation of coordination compounds," *Coordination Chemistry Reviews*, vol. 7, no. 1, pp. 81–122, 1971.

[28] R. N. Jadeja, S. Parihar, K. Vyas, and V. K. Gupta, "Synthesis and crystal structure of a series of pyrazolone based Schiff base ligands and DNA binding studies of their copper complexes," *Journal of Molecular Structure*, vol. 1013, pp. 86–94, 2012.

[29] M. Dolaz, V. McKee, A. Gölcü, and M. Tümer, "Synthesis, structural characterization, spectroscopic and electrochemical studies of N,N′-bis[(2,4-dimethoxyphenyl) methylidene]butane-1,4-diamine," *Current Organic Chemistry*, vol. 14, no. 3, pp. 281–288, 2010.

[30] R. C. Maurya, A. Pandey, J. Chaurasia, and H. Martin, "Metal nitrosyl complexes of bioinorganic, catalytic, and environmental relevance: a novel single-step synthesis of dinitrosylmolybdenum(0) complexes of $Mo(NO)2^6$ electron configuration involving Schiff bases derived from 4-acyl-3-methyl-1-phenyl-2-pyrazolin-5-one and 4-aminoantipyrine, directly from molybdate(VI) and their characterization," *Journal of Molecular Structure*, vol. 798, no. 1–3, pp. 89–101, 2006.

[31] Z.-Y. Yang, R.-D. Yang, F.-S. Li, and K.-B. Yu, "Crystal structure and antitumor activity of some rare earth metal complexes with Schiff base," *Polyhedron*, vol. 19, no. 26-27, pp. 2599–2604, 2000.

[32] K. Nakamato, *Infrared and Raman Spectra of Inorganic and Coordination Compounds*, Wiley-Interscience, New York, NY, USA, 5th edition, 1997.

[33] J. Liu, B. Zhang, W. U. Bowan, K. Zhang, and H. U. Shenli, "The direct electrochemical synthesis of Ti(II), Fe(II), Cd(II), Sn(II), and Pb(II) complexes with N, N′-bis(Salicylidene)-o-phenylenediamine," *Turkish Journal of Chemistry*, vol. 31, pp. 623–629, 2007.

[34] H. Naeimi and M. Moradian, "Synthesis and characterization of nitro-Schiff bases derived from 5-nitro-salicylaldehyde and various diamines and their complexes of Co(II)," *Journal of Coordination Chemistry*, vol. 63, no. 1, pp. 156–162, 2010.

[35] D. X. West, M. A. Lockwood, A. E. Liberta, X. Chen, and R. D. Willett, "Spectral nature, antifungal activity and molecular structure of metal complexes of acetylpyrazine ^{4}N-substituted thiosemicarbazones," *Transition Metal Chemistry*, vol. 18, no. 2, pp. 221–227, 1993.

[36] Y. Inada, K.-I. Sugimoto, K. Ozutsumi, and S. Funahashi, "Solvation structures of manganese(II), iron(II), cobalt(II), nickel(II), copper(II), zinc(II), cadmium(II), and indium(III) ions in 1,1,3,3-tetramethylurea as studied by EXAFS and electronic spectroscopy. Variation of coordination number," *Inorganic Chemistry*, vol. 33, no. 9, pp. 1875–1880, 1994.

[37] A. Bayri and M. Karakaplan, "Theoretical approach to the magnetic properties of Mn(II), Cr(III), and Cu(II) complexes in the newly reported 12- and 15-membered macrocyclic ligands," *Pramana*, vol. 69, no. 2, pp. 301–308, 2007.

[38] W. Ferenc, K. Czapla, and J. Sarzy, "Magnetic, thermal and spectral characterization of 2,4-dimethoxybenzoates of Mn(II), Co(II) and Cu(II)," *Eclética Química*, vol. 32, no. 3, pp. 7–12, 2007.

[39] P. P. Dholakiya and M. N. Patel, "Preparation, magnetic, spectral, and biocidal studies of some transition metal complexes with 3,5-dibromosalicylideneaniline and neutral bidentate ligands," *Synthesis and Reactivity in Inorganic and Metal-Organic Chemistry*, vol. 32, no. 4, pp. 819–829, 2002.

[40] S. A. Sallam, "Synthesis, characterization and thermal decomposition of copper(II), nickel(II) and cobalt(II) complexes of 3-amino-5-methylpyrazole Schiff-bases," *Transition Metal Chemistry*, vol. 30, no. 3, pp. 341–351, 2005.

[41] I. Pal, F. Basuli, and S. Bhattacharya, "Thiosemicarbazone complexes of the platinum metals. A story of variable coordination modes," *Proceedings of the Indian Academy of Sciences: Chemical Sciences*, vol. 114, no. 4, pp. 255–268, 2002.

[42] Y. Anjaneyulu and R. P. Rao, "Preparation, characterization and antimicrobial activity studies on some ternary complexes of Cu(II) with acetylacetone and various salicylic acids," *Synthesis and Reactivity in Inorganic and Metal-Organic Chemistry*, vol. 16, no. 2, pp. 257–272, 1986.

[43] B. Matthäus, "Antioxidant activity of extracts obtained from residues of different oilseeds," *Journal of Agricultural and Food Chemistry*, vol. 50, no. 12, pp. 3444–3452, 2002.

[44] M. N. Alam, T. B. Wahed, F. Sultana, J. Ahmed, and M. Hasan, "In vitro antioxidant potential of the methanolic extract of *Bacopa monnieri* L," *Turkish Journal of Pharmaceutical Sciences*, vol. 9, no. 3, pp. 285–292, 2012.

[45] R. M. S. Pereira, N. E. D. Andrades, N. Paulino et al., "Synthesis and characterization of a metal complex containing naringin and Cu, and its antioxidant, antimicrobial, antiinflammatory and tumor cell cytotoxicity," *Molecules*, vol. 12, no. 7, pp. 1352–1366, 2007.